

# Haptic Rendering of Cutting: A Fracture Mechanics Approach

Mohsen Mahvash and Vincent Hayward

Department of Electrical and Computer Engineering &  
Center For Intelligent Machines  
McGill University

3480 University Street, Montreal, Quebec, H3A 2A7 Canada  
{mahvash|hayward}@cim.mcgill.ca

## Abstract

Cutting a deformable body may be viewed as an interchange between three forms of energy: the elastic energy stored in the deformed body, the work done by a sharp tool as it moves against it, and the irreversible work spent in creating a fracture. Other dissipative phenomena such as friction can optionally also be considered. The force applied can be found by evaluating the work done by a tool which is sufficiently sharp to cause local deformation only. To evaluate this work, we propose a computational model that reduces cutting to the existence of three modes of interaction: deformation, rupture, and cutting, each of which considers the exchange between two forms of energy. During deformation, the work done by a tool is recoverable. During rupture, this work is zero. During cutting, it is equal to the irreversible work spent by fracture formation. The work spent in separating the sample is a function of its fracture toughness and of the area of a crack extension. It is in principle necessary to compute the deformation caused by a sharp tool in order to recover the force. This is in general an unsolved problem. However, for the case of a sharp interaction, measurements from tests performed on samples used in conjunction with analytical approximations to the contact problem, make it possible to propose a model which is applicable to haptic rendering. The technique is then compared to experimental results which confirms the model hypotheses. An implementation of the model that yields realistic results is also described.

## 1 Introduction

When the elements of virtual mechanical environments are assumed to be rigid, the problems

of haptic real-time simulation concern mostly collision detection, friction between bodies, multi-body dynamics, point-to-surface and surface-to-surface interaction, see for example [6], [7], [8], [14], [16], [20], [22], [26], [27], [30], [31]. When the elements of these environments are assumed to be soft, the simulation of deformation is required. This is generally computationally demanding. Assuming however that deformation is linear-elastic and that no changes occur in the discretization of a body, the linear superposition principle makes it possible to perform most computations in preprocessing for a given body [12], [20].

### 1.1 Difficulties with Simulation of Cutting

Virtual cutting has received little attention in the literature despite its potential importance for surgical simulators and other applications. Previous attempts made to address this subject relate mostly to modifications made to the simulation of deformation, and use similar computational approaches such as finite element methods (i.e. [28], [13], [10], [25]). With these techniques, cutting is assumed to take place when the force, or rather the stress, created by a tool during deformation reaches a threshold. The cutting process is typically simulated by eliminating one or several discrete elements from the virtual object, such as springs or tetrahedral regions. This makes it difficult to evaluate a force to be experienced by a subject holding a virtual cutting tool. One problem is to ensure mathematical continuity of the computations related to deformation, while the topology of the underlying mesh structure is changed. A physically based approach should at least satisfy the law of conservation of energy, a condition which is difficult to meet when modifying a mesh in real-time. Physically based approaches must also ensure that

the simulation results depend on measurable parameters and not on arbitrary choices. Mesh approaches do not meet this requirement since the mesh density, which by principle should be arbitrary, has a direct influence on the result.

Aside from the issues of real-time computing, the simulation of cutting with a sharp edge is itself not easy because it appeals both to contact mechanics and to fracture mechanics [4]. Numerical approaches such as finite element methods (FEM) and boundary element methods (BEM) break down as a result on their reliance on discretization of the geometry of a solid. They require far too many discrete elements to approximate a contact, compared to those needed to compute global deformation. Other possible approaches employ approximations of body geometries by standard cases such as half planes for contacts at uncut locations [18], or infinite wedges for contacts where a cut is already initiated [23]. It is then possible to solve the problems of deformation and contact analytically, but even then, the cases of sharp contacts are still open problems.

## 1.2 Stress Versus Energy Approaches

A body is cut, or rather, a crack or micro-crack (most materials or structural materials contain many pre-existing microscopic cracks) propagates under two well defined conditions, the first relates to stress and the second to energy. The stress condition states that the stress at the *tip* of a crack must exceed a certain value called “cohesive stress”. Stress is locally magnified at tip of a crack according to its shape, length, and orientation. This makes difficult to determine where and when the cohesive stress is reached. The energy condition states that sufficient energy must be supplied to extend a crack [1]. In fracture mechanics, the strength of a sample against fracture is often studied by applying the energy condition although it may not satisfy the stress condition. The energy approach yields different computational techniques to investigate the strength of materials and of structural materials [1]. Briefly, the change of elastic energy in a body undergoing fracture is related to the variation of the global stress field. The determination of this field can be complex in the case of a sharp contact, but it is also reasonable to ignore the change in elastic energy while a sharp cut is made because it must be small compared to the other two contributions to the total energy.

## 1.3 Sharp Interaction

The interaction between a body and a cutting tool involves different forms of the deformation problem: local, global, or even deformations which cannot be reduced to one of these forms. A wide range of contact areas can be considered: from the macroscopic scale to microscopic dimensions (cell walls for example). There are different forms of damage, from brittle fracture to plastic flow.

For purposes of cutting simulations, however, the most legitimate interaction cases should be considered first. These cases normally involve the creation of predictable and desirable cuts that cause the least damage possible (of interest for dissection, for example). This corresponds to using a tool which is sufficiently sharp to limit deformation to a small region around the contact area. We call such interaction a “sharp interaction”. Whether it is possible to approximate a general interaction by a sharp interaction depends on the sharpness of the tool edge, the sharpness of contact, the extensibility of the deformable body, and how the body is supported at its boundary. Clearly, sharp interactions depend strongly on the microscopic geometry of the tool edge and on proper support of the sample. The hallmark of sharp cuts is predictability.

The model introduced here is physically sound and represents materials and tools by a small number of parameters which can be easily identified from experimental tests, as later illustrated in this paper. It also affords the general advantages of physics-based simulation approaches in the sense that ranges of parameter values give rise to distinct behaviors observed in cutting tests performed under controlled conditions.

In Section 3, the concept of the work done by fracture is recalled. In Section 4, we combine the energy approach to fracture mechanics with local properties of sharp interactions to propose a physically based model capable of real-time computational prediction of sharp cutting. Experimental tests involving cutting samples of potatoes and of calf liver are described and discussed in Section 5. An implementation is presented in Section 6. The applicability and the limitations of the approach introduced in this paper are discussed in Section 7.

## 2 Related Work

A number of methods for haptic simulation of cutting have been researched, all in the framework

of surgery simulation. Song and Reddy described a technique for cutting linear elastic objects defined as finite element models [28]. Cutting takes place when the force exerted by the user exceeds the shear strength of the virtual object. The node at which cutting occurs is released and creates two new nodes. This technique was applied in two dimensions.

Delingette et al. consider cutting as a change in topology, which precludes directly using pre-computation as in their previous work [13], [25]. They propose a new model named “tensor spring” related to particle methods in order to achieve real-time simulation of cutting. It is a hybrid model which uses elastic modeling with pre-computations, yielding a tensed mass model with real-time ability. They simulate cutting by eliminating tetrahedral elements from the model.

Bro-Nilsen also simulates cutting by the removal of tetrahedral elements, combined with a technique for updating the pre-computed inverse of the stiffness matrix of finite element when cutting takes place [10]. At each time step, a stiffness matrix is found to be the sum of a previously computed matrix and a matrix containing a small number of nonzero values to account for the effect of a missing element. Then, the Woodbury formula is applied to compute the inverse of the updated matrix, thereby re-using the inverse of the previous one. However, the computational load is still too high for large number of mesh elements.

There exists other approaches to deal with the modeling of cutting forces, invariably independently from energy considerations. Tanaka et al. consider the cutting force to be a friction force between the rigid body and the tool related to velocity [29]. Basdogan et al. simulate the interaction force between cutting tool and body surface as a spring force proportional to indentation depth along surface normal and a damping force proportional to tangential velocity [5].

For global deformations, several techniques have been proposed to reduce the computation time required for simulation. Astley and Hayward proposed using a multi-layer FE mesh which can accommodate nonlinear behaviors. A body is represented by a hierarchical mesh related by Norton equivalents [3]. Bro-Nielson and Cotin described a condensation technique in FEM [9]. The computation time can be reduced to the computation time of a model involving only the surface nodes of the

mesh. James and Pai applied boundary element method which also only needs surface mesh [19]. Cotin et al. introduced the idea of pre-processing for computation of deformation in linear-elastic materials [12]. Zhuang and Canny considered the effects of large deformations [32].

### 3 Work Done by Fracture

When a deformable body is elastically loaded as in Figure 1a, all the work done to deform it is stored. Upon unloading the body returns to its initial shape and the elastic energy is entirely recovered. Figure 1b shows the same body in which a crack is created during loading. For each displacement, the unloading force is smaller than the loading force. The shaded area corresponds to the irreversible work consumed to create the crack [4].

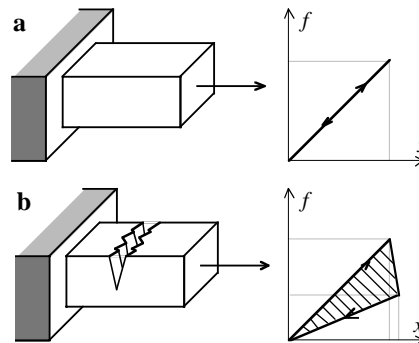


Fig. 1. Work done **a)** in the deformation, and **b)** in the fracture of a body.

In the case of elastic fracture (i.e. fracture in which plastic deformation in the body limited to a small region near the crack), the work required to propagate a crack of unit of area inside a body is specific to a material or structural material and is called its fracture toughness  $J_c$ . Like other properties such as the elastic modulus, fracture toughness can vary with the temperature, the environment, aging, orientation and so-on. In the quasi-static case (kinetic energy is neglected), the irreversible work done to fracture a body is entirely consumed by the crack formation [4]. Given a crack  $s$  of area  $a(s)$ , this work is given by:

$$W_s = J_c a(s). \quad (1)$$

Consider now the case of a sharp tool propagating a crack without friction and causing negligible elastic energy to be stored. As exemplified

in Figure 2, the shaded area inside a closed force-displacement response represents the irreversible work done while creating the cut. In the case of a quasi-static linear fracture, this work is related to the fracture toughness of the body and to the size of a crack extension of length  $l$  and depth  $x$ :

$$W_s = J_c l x. \quad (2)$$

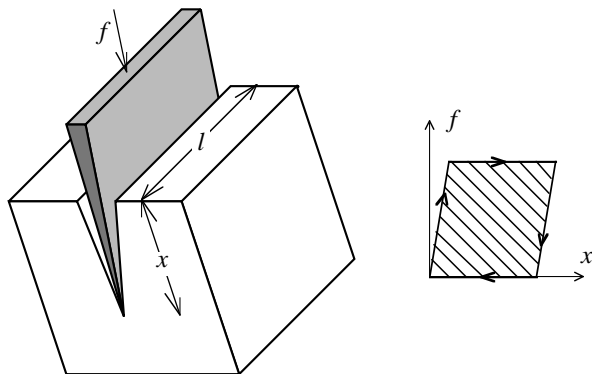


Fig. 2. Work done while cutting.

In [4], cutting tests of prepared samples is shown to be a powerful method to determine the fracture toughness of extensible structural bio-materials which do not lend themselves to standard test methods.<sup>1</sup> These tests must be performed with sharp tools that can guarantee the elastic energy stored in the body to be much smaller than the irreversible work spent in creating a fracture, thereby limiting the measurement error.

This approach can be adopted to evaluate the tool force during haptic rendering of a sharp interaction, where in steady state, the tool work equals the work of fracture. It requires the knowledge of material toughness and avoids the need to accurately compute deformation in order to predict the extension of a crack. This is developed in the next section.

## 4 Model for Sharp Interaction

A sharp interaction generally involves two macroscopically distinct phenomena: *deformation* and *fracture*. Before these can be defined, some assumptions are needed:

<sup>1</sup>Atkins et al. measured the fracture toughness of selected structural biomaterials. The values that they found make it clear that fracture toughness is a property of these material that is quite unrelated to their stiffness. In units of kJ/mm; bone: 2, rabbit skin: 20, apple: 6, potato: 0.2, muscle (perimysial tracts): 0.5 to 1.0.

1. The body under consideration is assumed to be initially free from any residual internal stress and from external loading.
2. Purely elastic deformation is assumed to occur in the entire body except in a small region around the crack front where elastic fracture occurs.
3. The displacement of the tool is normal to the contact surface between the tool and the body. When the contact is located at the end of a cutting crack (a crack already created by cutting, or otherwise), the tool displacement is along a fixed cutting axis with no rotations. The displacement of the contact edge defines a cutting plane.

### 4.1 Cutting Force

Figure 3 shows two states of a cutting process separated by a short time interval  $\Delta t$ . Fracture is defined in terms of surface change, that is, in terms of the spread of surface  $s^+$  (one wall of the crack) to  $s^+ + \Delta s^+$  and of surface  $s^-$  (the other wall) to  $s^- + \Delta s^-$  in  $R_{s+\Delta s}$ . Deformation, on the other hand, refers to the change of body shape  $R_s$  to  $R_{s+\Delta s}$  as a result of elastic deformation.

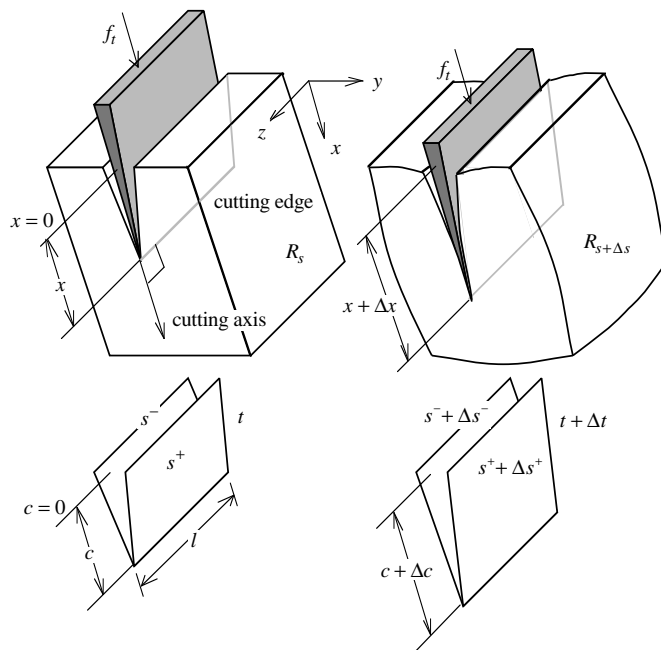


Fig. 3. Definition of a cutting process:  $x$  measures the tool displacement and  $c$  the crack extent. The difference is the local deflection.

Accounting for all energy terms entering an energy balance equation, the law of energy conservation applied between two consecutive states at

times  $t$  and  $t + \Delta t$  yields:

$$\Delta W_e = \Delta U + \Delta W_s, \quad (3)$$

where  $\Delta U$  is the change of elastic potential energy stored in  $R_s$  and  $R_{s+\Delta s}$ :  $\Delta U = U_{R_{s+\Delta s}} - U_{R_s}$ ,  $\Delta W_e$  is the external work applied by the tool during the change from  $R_s$  to  $R_{s+\Delta s}$ , and  $\Delta W_s$  is the irreversible work of fracture. For a quasi-static fracture, calling  $a(\Delta s)$  the area of  $\Delta s$ :

$$\Delta W_s = J_c a(\Delta s). \quad (4)$$

$\Delta W_e$  is a function of the tool displacement,  $\Delta x$ , and of the force  $f_t$  it applies:

$$\Delta W_e = f_t \Delta x. \quad (5)$$

From the second assumption, the tool displacement and the tool force are vectors normal to the contact surface. Substituting Equations (4) and (5) into Equation (3) gives:

$$f_t = \frac{\Delta U}{\Delta x} + \frac{J_c a(\Delta s)}{\Delta x}. \quad (6)$$

## 4.2 Modes of Interaction

The entire process of a sharp interaction can be reduced to three possible modes defined by equating one of the three terms of the energy balance equation to zero.

**Deformation** ( $\Delta W_s/\Delta x = 0$ ). In this mode, no separation occurs, so  $\Delta s = 0$ . A deformation mode for sharp interaction can be subdivided into two states, distinguishing between places that had already been cut and those that had not, that is, whether a crack pre-exists or does not.

Referring to Figure 4a, State 1 represents a deformation problem when the loading is reduced to the contact of an object of a given geometry with an infinite half plane. There exists analytical solutions for some tool geometries. Numerical approaches to compute the elastic contact for any tool geometry also exist [21]. A sharp tool, however, may cause large deformation and plasticity around the zone of contact. If it is acceptable to represent the body geometry by a half plane, a small set of deformation measurements for a given tool will be sufficient to solve the deformation problem for any body shape. For a sharp interaction with uniform deflections around a contact line, we also assume that the shear along contact line can be neglected.

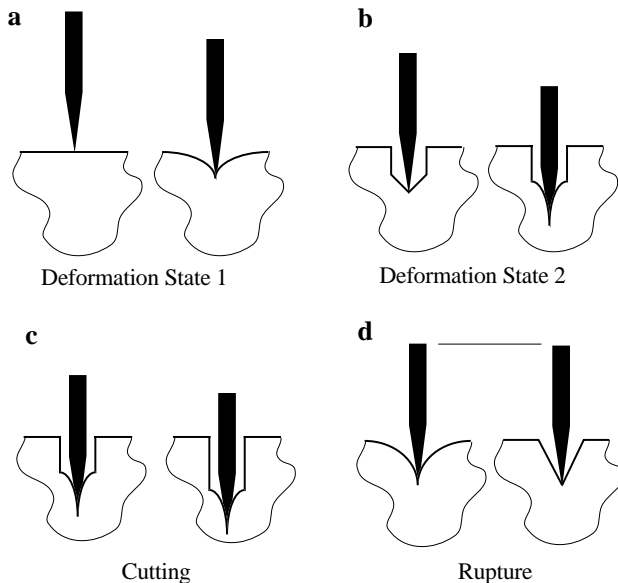


Fig. 4. Tool-body interaction modes. Legend: a wavy line indicates a region subject to global deformation; a straight segment symbolizes a wall of the original body or a wall created by fracture; a curved segment symbolizes a wall subject to deformation. As these phenomena may occur at various scales, a precise sense of scale is not implied in the figure.

This is similar to the approximation used in contact mechanics when the contact problem cannot be solved. This makes it possible to extend the result of measurement for a uniform line contact of unit of length, to any length of line contact. Calling  $\delta$  the local deflection of the body,  $f_1$  represents the force deflection response measured for a line of contact of unit length:

$$f_t = l f_1(\delta). \quad (7)$$

State 2 of Figure 4b represents a different contact problem. The effect of a crack formation is to shrink the deformation of the body to a small zone around the edge, where the tool displacement is along the cutting axis. The geometry of the body as well as the crack length can be ignored. Therefore, a set of cutting tests should be sufficient to solve the problem of deformation of any body shape and cutting any crack length. Calling now  $f_2$  the force deflection response measured for a line contact of unit of length:

$$f_t = l f_2(\delta). \quad (8)$$

For haptic rendering purposes, an important factor for realism is stability. At high stiffness, a unilateral interaction can create limit cycles similar to those that occur in the case of simulated contact with hard objects. It is known that fast update rates of the rendered force and some device damping can be sufficient to quench them [11].

**Cutting** ( $\Delta U/\Delta x = 0$ ). In this mode, during the displacement of a cutting tool and without change in the total elastic energy stored in the body, the deformed region around the cutting edge shifts to a new contact location as in Figure 4c. Since  $\Delta W_e = \Delta W_s$ , the force applied by the tool is given by:

$$f_t = \frac{\Delta W_s}{\Delta x} = \frac{J_c a(\Delta s)}{\Delta x}. \quad (9)$$

The shape of  $\Delta s$  can be estimated from observations based on the tool shape. For instance, in the case of a line cut with a thin knife,  $\Delta s$  can be considered to be rectangular with length  $l$ , and width  $\Delta x$ :

$$f_t = J_c l. \quad (10)$$

**Rupture** ( $\Delta W_e/\Delta s = 0$ ). In this mode represented by Figure 4d, the tool does not exchange any energy with the body. The stored elastic energy instantaneously creates a crack  $\Delta s$ , with  $\Delta t = 0$ . The area of  $\Delta s$  can be evaluated to be

$$a(\Delta s) = \frac{\Delta U}{J_c}. \quad (11)$$

The shape of  $\Delta s$  could again be estimated from observations on rupture.  $a(\Delta s)$  can however be estimated from another approach. Here, it can be assumed that a rupture mode always switches to a cutting mode. This defines  $a(\Delta s)$  for a given  $\Delta s$ . However, this approach can be used only where  $a(\Delta s)$  is smaller than that predicted by Equation 11. This means that the stored elastic energy is sufficient to create a crack that defines the transition from deformation in State 1 to a cutting mode associated to deformation in State 2.

### 4.3 Interaction Modes Sequence

Figure 5 summarizes the interaction modes and the transition conditions between them in terms of the deflection responses  $f_1(\cdot)$  and  $f_2(\cdot)$ ,  $f_r$  the force at which a rupture occurs, and  $J_c$ , the toughness of the body.  $x$  represents the displacement of the

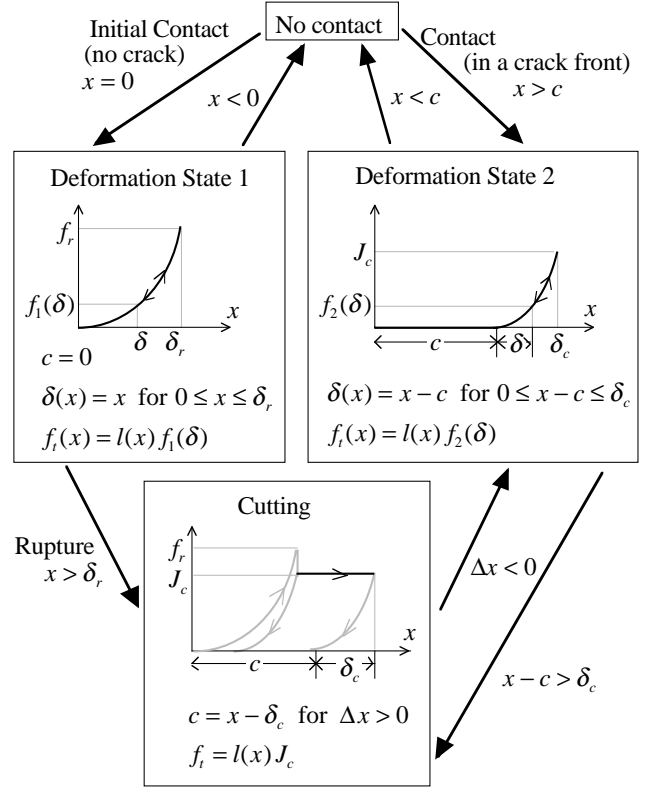


Fig. 5. Possible sequences of interaction modes.

tool and  $c$  the extent of the crack, as depicted by Figure 3.

A collision at an uncut location determines the beginning of a deformation mode in State 1. The interaction remains in this mode as long as the tool is in a contact with the body ( $x \geq 0$ ), and as long as the local deflection is smaller than  $\delta_r$ , the deflection at which a rupture occurs, and which is such that  $f_r = f_1(\delta_r)$ . At the rupture point, a switch to the cutting mode occurs with a crack of extent  $c = x - \delta_c$  where  $\delta_c$  is a deflection such that  $J_c = f_2(\delta_c)$ . In other words,  $\delta_c$  is the deflection in deformation State 2 corresponding to the formation of a crack. It stays in this mode as long as the tool moves inside the body ( $\Delta x \geq 0$ ), otherwise the interaction mode switches to a pure deformation mode in State 2.

When the tool contacts the body at a location which has already been cut (inside a crack front), a deformation mode in State 2 begins and continues as long as the tool is in a contact with the body ( $x > c$ ), and as long as the local deflection is smaller than  $\delta_c$ . For a tool displacement that causes a deflection greater than  $\delta_c$ , the interaction switches back to a cutting mode, wherein the crack

length extends with the tool displacement, that is  $\delta = \delta_c$ .

## 5 Experiments

A series of cutting tests on samples were carried out under controlled conditions to test the model hypotheses:

- Displacement-force curves should be repeatable and should resemble each other for the same cutting conditions and similar samples. This would indicate that cutting processes can be predicted.
- The existence of three distinct regimes should be observed, corresponding to at least three tool-body interaction modes discussed in Section 4.2, namely deformation, rupture, cutting, as well as the existence of switching conditions between them, independently from epiphenomena involving friction and variations due to sample inhomogeneity or anisotropy.
- The dependency of the cutting force on contact length should be observed.

### 5.1 Materials and Methods

The tests involved cutting precisely shaped prismatic samples of two different biomaterials: potato and fresh calf liver. These samples were bonded by one face to a solid metallic plate using a cyanoacrylate adhesive which is capable of long term bonding even to moist objects. This provided a traction surface, free of residual stresses. One potato sample was a rectangular prism, 15 mm deep, 20 mm wide, and 40 mm long. Another sample was a triangular prism forming wedges 17 mm deep, 18 mm wide at the base, and 50 mm long. The liver sample was a rectangular prism 10 mm deep, 20 mm wide, and 90 mm long.

A robot manipulator holding a sharp razor blade was used to perform cutting in a direction orthogonal to the axes of the prisms. It was programmed to cut at one mm/s with a blade firmly clamped to the manipulator’s terminal link. The manipulator configuration was optimized to minimize the effect of link and drive flexibility (see Figure 6). The resulting force was measured in-situ, on the load path between the blade and the manipulator’s terminal link. These facilities were conveniently provided by ACME, the Active Measurement Facility developed at the University of British Columbia by Pai and co-workers [24].

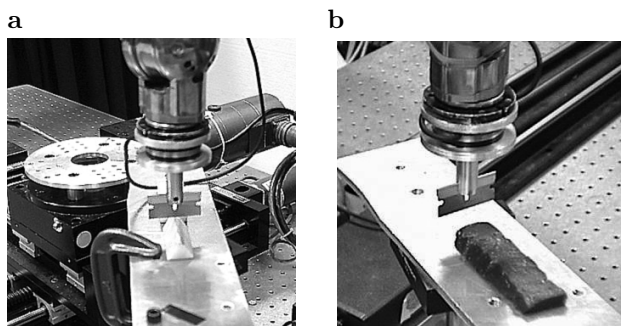


Fig. 6. ACME’s manipulator performing a) potato wedge cutting, b) liver sample cutting.

### 5.2 Results

Figures 7a-8a show robot displacement trajectories, and Figures 7b-8b each show one example of force trajectory, for the cases of potato samples of rectangular section and of triangular section respectively. The same data in the form of overlaid displacement-force phase curves resulting from cutting the same sample are collected in Figures 7c-8c (three curves for the rectangular section, two curves of the triangular section).

Figure 9a shows a position trajectory and Figure 9b an example of force trajectory for the case of a liver sample. Figure 9c collects three overlaid displacement-force phase curves for cuts made on the same sample. The average of these three responses is shown in Figure 9d.

### 5.3 Discussion

The results support the hypothesis that the cutting process can be reduced to switching between three regimes corresponding to different tool-sample interaction modes.

Referring to Figures 7c-8c (potato samples), a deformation regime starts at (1) with a collision between the blade and the sample after which elastic energy accumulates in the sample. The rupture, from (2) to (3), occurs in less than 50 ms, almost instantaneously as the release of elastic energy creates a crack. The process then switches to cutting at (3), where the work performed by the blade separates the sample without change in deformation energy. Equation 10 predicts that the tool force is constant for a sample with a rectangular section (Figure 7c), and that it increases with the contact length in the case of a triangular section (Figure 8c). The results clearly indicate the dependency of the cutting force on the contact

length between the cutting edge and the sample. Another deformation mode begins at (4) when the blade velocity reverses, and ends at (5). The small force reversal there is probably due to friction. It is maximum at zero velocity, when the walls of the crack exert the largest pressure, and then vanishes during retreat.

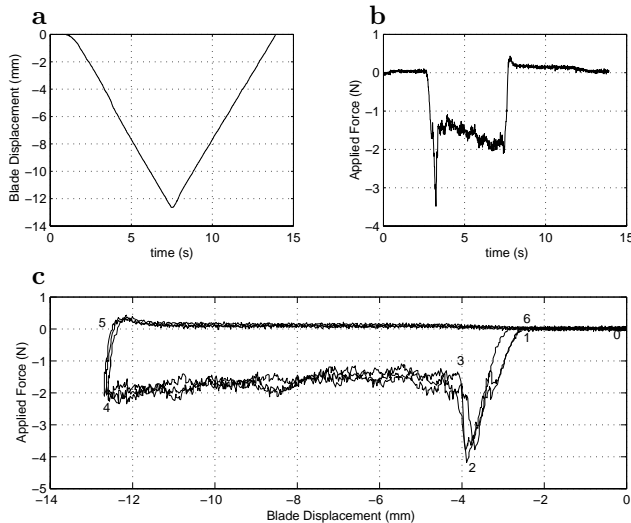


Fig. 7. Displacement and force during cutting rectangular potato prisms.

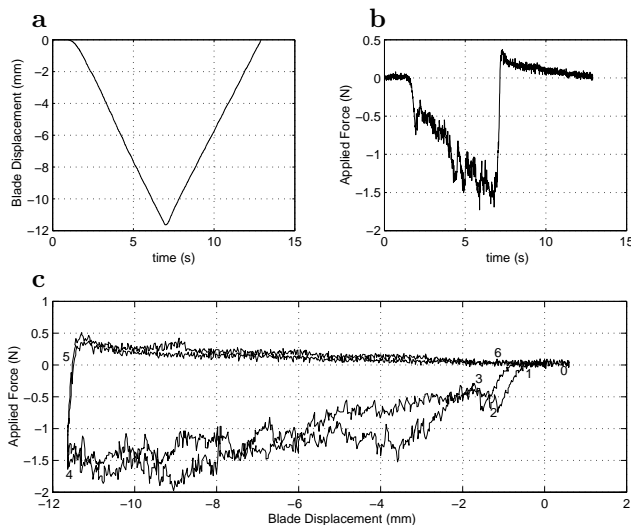


Fig. 8. Displacement and force during cutting triangular potato prisms.

The curves show a considerable difference between the deformation regime from (1) to (2), that is, of initial indentation of an uncracked sample, compared to that (4) and (5), that is, of retreat from a crack. The deformation energy, the defor-

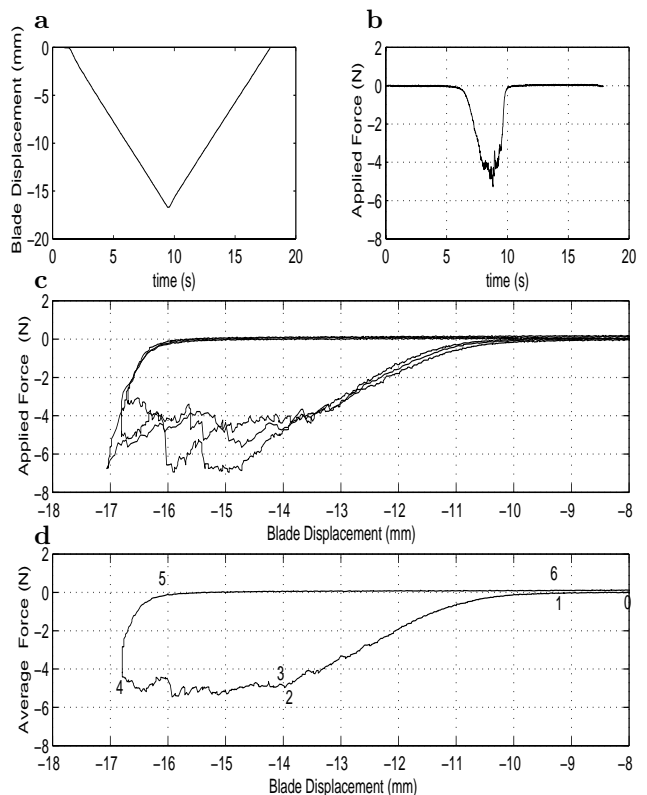


Fig. 9. Displacement and force during cutting liver samples.

mation depth, and the rate of change of force all differ. It is likely that the force variations at various scales result from inhomogeneities in the sample and/or small changes in the contact conditions.

In the case of liver samples, Figure 9, it is apparent that the response to cutting is not as predictable as it is for potatoes. The reduced predictability is probably the result of the micro-behavior of liver tissue which is such that small changes in the contact mechanics yield significant changes in the stress condition. It is also likely that micro-cracks are not distributed as evenly in liver as they are in potatoes. In addition, fracture toughness may be more variable. These results are indicative of the fact that a cutting process always exhibits some amount of stochastic behavior and that this aspect is more pronounced for certain tool/tissue pairs.

Whether one or combination of these three factors dominate in this example, it is nevertheless true that the stochastic component of a response to cutting is always reduced with sharper tools. It is well known that tool sharpness generally determines the predictability of a cut, since the size of

the contact depends highly on its micro-geometry. The stochastic nature of the behavior is made evident in the averaged response. With just three cuts made a few millimeters apart, the average response during the cutting phase becomes almost flat. These observations may have important consequences for the design of surgical simulators capable of haptically rendering cuts.

The liver results, like those obtained from potatoes, clearly indicate the existence of different deformation modes corresponding respectively to the initiation of a cut or to the retreat from a crack. Also, the transition from a deformation mode to a cutting mode does not yield a significantly discontinuous response, as it was the case for potato samples. This preliminary study is not sufficiently detailed to allow us to conclude whether this absence of discontinuity can be attributed to plastic deformation, since other factors could explain it.

## 6 Implementation

The model described in Section 4 was implemented in a computer to simulate cutting in real time. The forces computed as a function of displacement were rendered by a PenCat/Pro™ haptic device (Immersion Canada Inc.) which can render forces in two dimensions. The simulation program consisted of two independent real-time threads running under RTLinux 3.0. The first execution thread computed the cutting force at a self adjusting rate according to the complexity of the rendering (typically 1 kHz). The other thread ran at 2 kHz to drive the haptic device. A separate user process provided for graphics and user interaction with Tcl/Tk.

During simulation, the virtual knife was kept at a constant orientation. The virtual body consisted of two layers with different toughness which could be independently changed for each case. Setting the two sets of parameters to the same values would simulate an homogenous body. The graphical user interface can be seen in Figure 10. It was assumed that both layers had the same force deflection responses.  $f_1$  and  $f_2$  were represented by two virtual walls which could be independently adjusted. The response could be linear, quadratic, or cubic,  $f_1(\cdot) = f_r [./\delta_r]^i$ , and  $f_2(\cdot) = J_c [./\delta_c]^j$ , with  $i$  or  $j = 1, 2$ , or  $3$ .

The force returned by the haptic device consisted of three components which were computed separately before being added: the force representing a

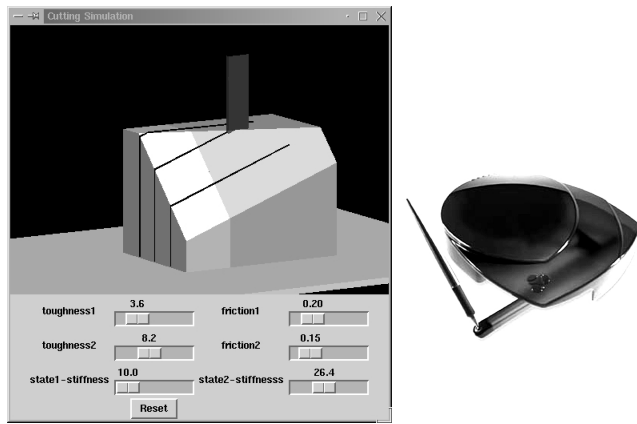


Fig. 10. Graphical user interface and device used in the cutting simulation.

sharp interaction, the lateral force experienced by the knife, and a friction forces. The lateral force experienced by the knife was modeled empirically as an elastic wall that kept the knife displacement along the cutting axis. The friction force due to sliding contacts between the knife sides and the body, as well as the friction force due to sliding contacts between sharp edge of knife and uncut body made was also modeled empirically using the method of [16] (Section 3.1), whereby the friction force is predicted in terms of presliding displacements. The cutting force algorithm for the case of one single material is summarized in Figure 11.

Figures 12 and 13 shows simulated displacement-force curves created by virtually cutting by hand homogeneous blocks where the various body-tool interaction regimes have been labeled as in the experimental curves of Section 5. The parameters were set manually for best empirical match. The irregularities during cutting are due to small movements of the virtual tool, causing switching between deformation and cutting. The machine used to perform the tests was many times more rigid than a human hand.

## 7 Conclusion

### 7.1 Summary

Sharp cut interactions were defined in terms of concepts from contact and fracture mechanics, whereby a body is locally deformed before it is separated. For purposes of haptic rendering, a sharp tool was assumed to make a straight or curved line of contact with a deformable body. The model introduced an energy approach inspired from frac-

```

// Homogenous body and single cutting crack. Quantities related
// to gross geometry, Collision(Body, Tool), l(x) from other process.
// l(x) can be approximated by l(CrackLength) if severe lack of synchronization.

```

```

begin thread
  if (¬CuttingFrameKnown ∧ ¬Collision(Body, Tool))
    Fi ← 0
    exit
  fi
  if (¬CuttingFrameKnown ∧ Collision(Body, Tool))
    DefineCuttingFrame(ToolPosition, LocalSurfaceNormal)
    CuttingFrameKnown ← True
    CrackLength ← 0
    Deformation ← State1
  fi
  if CuttingFrameKnown
    [x, y] ← MapToCuttingFrame(ToolPosition) // local coordinates
    if x < 0
      CuttingFrameKnown ← False
      Fi ← 0
    else
      case Deformation = State1
        if x < δc // deformation
          δ(x) ← x
          fx ← l(x) f1(δ(x)) // f1 unilateral wall
          fy ← Friction([x, y], fx, μ)
        else // rupture
          CrackLength ← x - δc
          fy ← -LateralStiffness y // bilateral wall
          fx ← l(x) Jc + Friction([x, y], fy, μ)
          Deformation ← State2
        fi
        Fi ← MapToDeviceCoordinates([fx, fy])
      case Deformation = State2
        if x < CrackLength
          fx ← 0 // no contact
        else
          if x < δc + CrackLength // deformation
            δ(x) ← x - CrackLength
            fx ← l(x) f2(δ(x)) // f2 unilateral wall
          else // cutting
            CrackLength ← x - δc
            fx ← l(x) Jc
          fi
        fi
        fy ← -LateralStiffness y // bilateral wall
        fx ← fx + Friction([x, y], fy, μ)
        Fi ← MapToDeviceCoordinates([fx, fy])
      fi
    fi
  fi // Frame known
end thread

```

Fig. 11. Cutting algorithm expressed in pseudo code.

ture mechanics methods to evaluate the tool force given tool displacement. This made it possible to reduced the problem of cutting to the existence of three distinct interaction modes and to switching conditions between these modes over time. Measurements were required to define each mode completely, as a function of materials and tool conditions.

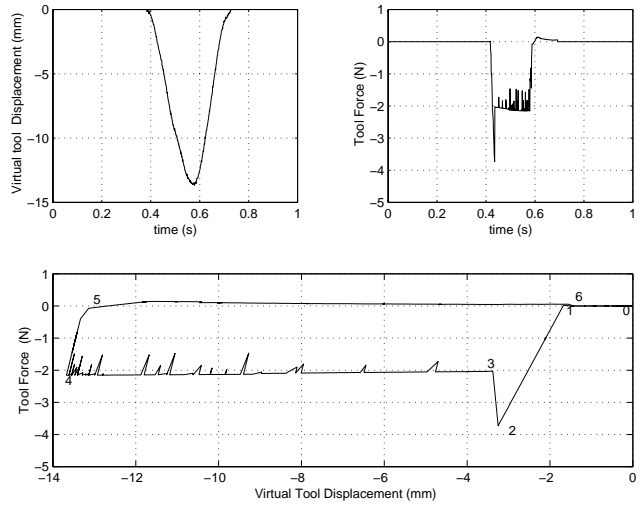


Fig. 12. Displacement and force during cutting simulation of potato.

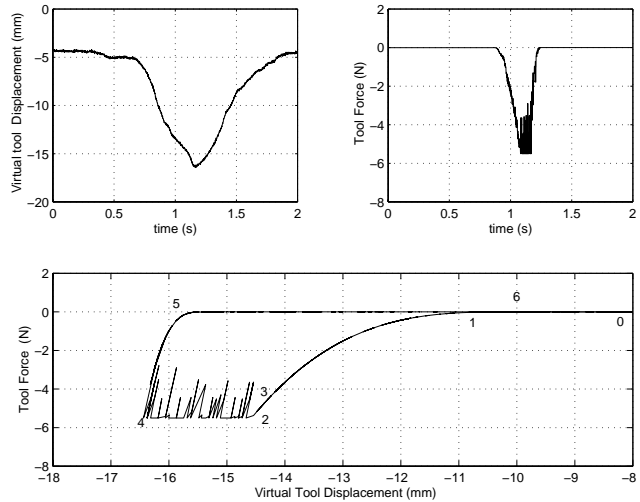


Fig. 13. Displacement and force during cutting simulation of liver.

Unlike the potato samples, the liver sample had deflection responses that could vary significantly. Liver was also more prone to yielding results having a significant stochastic component during the cutting mode. This may have important consequences for the design of surgical simulators that can render cuts with some fidelity.

A computer implementation of the model was described that could predict effectively the deterministic behavior of cutting in terms of material fracture toughness (energy per unit of area), local deflection responses per unit of length, and a rupture threshold per unit of length.

The model is computationally efficient. It is not limited to interaction between a uniform line

of contact and a deformable body of pre-defined shape. For the simulation of a sharp interaction with a body of arbitrary shape, the local cutting frame set at the location of initial contact serves to define subsequent interactions. The deflection is distributed over the length of the contact line, so the individual contacts can experience simultaneous but different interaction modes. The total tool force is then obtained by integration over the length. This integral may be obtained numerically from the contributions of discrete segments using data obtained from standard tests. The display of the resulting forces and torques would require the use of high fidelity haptic devices with torque rendering capability such as Freedom-7 [17] or its commercial version.<sup>2</sup>

## 7.2 Open Issues

The model should be extended to consider other tool movements, for example movements having rotations around the contact line. Additional measurements would be needed to obtain the deformation response in these cases. An important sub-case is that of a sliding contact, a case that we normally describe as a sawing movement. Whether sawing has a significant effect during cutting is an still an open question. The energy approach introduced in this paper might still be applicable to haptic rendering with sawing motion. Tests are being designed to determine how the tool work distributes among the force components involved in a sawing interaction, and whether the work of fracture is changed or not.

When materials are highly extensible, the force deflection response for the two states of deformation can be only known from samples which have comparable sizes and traction at the boundary. More research is needed to determine the sensitivity of these parameters on a cut, particularly in the case of pre-deformed extensible biomaterials.

The contact of the sides of a tool inside a crack made in deformable body was modeled empirically. More detailed models should account for the variation of friction according to global deformation. This was noticeable in potato cuts. However, the approaches already mentioned for simulation of deformation are applicable when the contact area is not small. The multi-layer approach described in [2] would make this possible.

<sup>2</sup><http://www.mpb-technologies.ca>

Viscoelastic effects have been ignored due to the low rates involved. However, the key assumptions needed to apply the energy approach, namely sharp interaction, approximations of contacts mechanics, and knowledge of fracture toughness, are not limited to purely elastic bodies. The same computational approach could be extended to include terms related to viscosity, and perhaps more importantly, to plasticity. Whether or not these terms need to be considered depends on the application.

The issues related to multi-modal, graphic and haptic, simulation have been side stepped because the determination of the force response appeals to techniques that are very different from that needed to determine the visual aspect of a simulation, and hence should rely on different representations. However, some aspects can be shared by the two modes, in particular the determination of collisions and of the contact position and length should use techniques developed for graphics, whereas the graphics could benefit from the knowledge of crack extensions with high spatial and temporal resolution that current graphics methods do not allow.

## 8 Acknowledgements

The authors thank J. E. Lloyd from the University of British Columbia for setting up the ACME facility in order to perform cutting tests and to provide us with the results. This paper benefitted from insightful comments from Claude Lacoursière of Critical Mass Labs, Montréal, Canada, Michel Audette of the Surgical Assist Group, AIST, Japan, and Oliver Astley of General Electric, Schenectady, NY, US.

This research is funded by the project “Reality-based Modeling and Simulation of Physical Systems in Virtual Environments” supported by IRIS-III, the Institute for Robotics and Intelligent Systems which is part of Canada’s Network of Centers of Excellence program (NCE). Additional funding is provided by NSERC, the Natural Sciences and Engineering Council of Canada, in the form of an operating grant for the second author.

## References

- [1] Anderson, T. L., 1995. *Fracture Mechanics: Fundamentals and Application*, 2nd ed. Boca Raton: CRC Press.
- [2] Astley, O., Hayward V., 2000. Design constraints for haptic surgery simulation. *Proc. IEEE Int. Conference on Robotics and Automation*, pp. 2446–2451.
- [3] Astley, O., Hayward, V., 1998. Multirate haptic simulation achieved by coupling finite element meshes through

- norton equivalents. *Proc. IEEE Int. Conf. on Robotics and Automation*, 1998. pp. 989–994.
- [4] Atkins A. G., Mai Y-W., 1985. *elastic and plastic fracture: metals, polymers, ceramics, composites, biological materials*, Chichester : Ellis Halsted Press.
- [5] Basdogan C., Ho, C., Srinivasan, M. A., 1999. Simulation of tissue cutting and bleeding for laparoscopic surgery using auxiliary surfaces. Proceeding of the *Medicine Meets Virtual Reality VII* Conference, San Francisco, CA.
- [6] Berkelman, P.J. Hollis, R.L., and Baraff D., 1999. Interaction with a Realtime Dynamic Environment Simulation using a Magnetic Levitation Haptic Interface Device. *Proc. IEEE Int. Conf. on Robotics and Automation*, pp. 3261-3266.
- [7] Brown, J. M., Colgate, J. E., 1997. Passive implementation of multi body simulation for haptic display. *Proc. International Mechanical Engineering Congress and Exhibition*, Dallas, TX, ASME, DSC-61, pp. 85–92.
- [8] Chang, B., Colgate, J. E., 1997. Real-time impulse-based simulation of rigid body systems for haptic display. *Proc. ASME, Dynamic Systems and Control Division*, Vol. 61, pp. 1–8.
- [9] Bro-Nielsen, M., Cotin, S. 1996. Real-time volumetric deformable models for surgery simulation using finite element and condensation. *Proc. Eurographics '96 - Computer Graphics Forum*, 15, pp. 57–66.
- [10] Bro-Nielsen, M., 1998. Finite element modeling in surgery simulation. *Proceedings of the IEEE*, 86:3, pp. 490–503.
- [11] Colgate, J. E., Brown, J. M., 1994. Factors affecting the z-width of a haptic display. *Proc International Conference on Robotics and Automation*, San Diego, CA, IEEE, Vol. 4, pp. 3205–10.
- [12] Cotin, S., Delingette, H., Ayache, N. 1999. Real-time elastic deformations of soft tissues for surgery simulation. *IEEE Transactions on Visualization and Computer Graphics*, 5:1, pp. 62–73.
- [13] Delingette, H., Cotin, S., Ayache, N. 1999. A hybrid elastic model allowing real-time cutting, deformations and force-feedback for surgery training and simulation. *Computer Animation Proceedings*, pp. 70-81.
- [14] Gregory, A., Lin, M., Gottschalk, S., and Taylor, R., 1999. H-Collide: A framework for fast and accurate collision detection for haptic interaction. *Proc. IEEE Virtual Reality Conference*.
- [15] Fritz, P. J., Barner, K., E. 1996. Stochastic Models for Haptic Texture. *Proc. SPIE Symposium on Intelligent Systems and Advanced Manufacturing - Telemanipulators and Telepresence Technologies III Conference*.
- [16] Hayward, V., Armstrong, B., 2000. A new computational model of friction applied to haptic rendering. In *Experimental Robotics VI*, P. I. Corke and J. Trevelyan (Eds.), Lecture Notes in Control and Information Sciences, Vol. 250, Springer-Verlag, pp. 403-412.
- [17] Hayward, V. Gregorio, P. Astley, O. Greenish, S. Doyon, M. Lessard, L. McDougall, J. Sinclair, I. Boelen, S. Chen, X. Demers, J.-P. Poulin, J. Benguigui, I. Almey, N. Makuc, B. Zhang, X. 1998. Freedom-7: A High Fidelity Seven Axis Haptic Device With Application To Surgical Training. In *Experimental Robotics V*, Casals, A., de Almeida, A. T. (eds.), Lecture Notes in Control and Information Science 232, pp. 445-456.
- [18] Hills D. A., Nowell D., Sackfield A., 1993. *Mechanics of elastic contacts*. Oxford, [England]; Boston, Butterworth-Heinemann.
- [19] James D. L. and Pai D. K., 1999. ArtDefo, accurate real time deformable objects. *SIGGRAPH 99 Conference Proceedings*. pp. 65–72.
- [20] James, D. L., Pai D. K., 2001. A unified treatment of elastostatic and rigid contact simulation for real time haptics. *Haptics-e, the Electronic Journal of Haptics Research*. Vol. 2, No. 1.
- [21] Johnson, K. L., 1987. *Contact mechanics*. Cambridge University Press.
- [22] Nahvi, A., Nelson, D.D., Hollerbach, J.M., and Johnson, D.E., 1998. Haptic manipulation of virtual mechanisms from mechanical CAD designs. *Proc. IEEE Intl. Conf. Robotics and Automation, Leuven, Belgium*, pp. 375–380.
- [23] Noller, B.M., 1972. Some contact problems for an elastic infinite wedge. *Journal of Applied Mathematics and Mechanics*, pp. 146–152, Vol 36(1).
- [24] Pai D. K., Lang J., Lloyd J. E., Woodham, R. J., 2000. ACME, a telerobotic active measurement facility. In *Experimental Robotics VI*, P. I. Corke and J. Trevelyan (Eds.), Vol. 250 of Lecture Notes in Control and Information Sciences, pp. 391–400, Springer-Verlag.
- [25] Picinbono, G., Lombardo, J.-C., Delingette, H., Ayache, N., 2000. Anisotropic elasticity and force extrapolation to improve realism of surgery simulation. *Proc. IEEE Conf. on Robotics and Automation, Proceedings*. Vol.1, pp. 596–602.
- [26] Ruspini, D., Khatib, O. 2000. A framework for multi-contact multi-body dynamic simulation and haptic display. *Proc. 2000 IEEE/RSJ International Conference on Intelligent Robots and Systems*.
- [27] Salcudean, S. E., Vlaar, T.D., 1997. On the emulation of stiff walls and static friction with a magnetically levitated input/output device. *J. Dyn. Syst. Meas. Contr.*, 119:127-132.
- [28] Song, G. J., Reddy, N. P., 1995. Tissue cutting in virtual environments. In *Interactive Technology and the New Paradigm for Healthcare*, Satava, R. M., Morgan, K., Sieburg, H. B. , Mattheus, R., and Christensen, J. P. (Eds.), Studies in Health Technology and Informatics, Chap. 54. IOS Press.
- [29] Tanaka, A., Hirota, K., Kaneko, T. 1998. Virtual cutting with force feedback. *Proc. Virtual Reality Annual International Symposium*, Vol. 199:8, pp. 71–7.
- [30] Yoshikawa, T, Yokokohji, Y., Matsumoto, T., Zheng, X-Z. 1995. Display of feel for the manipulation of dynamic virtual objects. *J. Dyn. Syst. Meas. Contr.*, 117:554–550.
- [31] Zilles, C. B., Salisbury, J. K., 1995, A constraint-based god object method for haptic display. *Proc. IEEE Int. Conf. Intel. Rob. and Syst.*, Vol. 3, pp. 146–151.
- [32] Zhuang, Y., Canny, J. 2000. Haptic interaction with global deformations. *Proc. IEEE Robotics and Automation Conference*, IEEE, Vol.3, pp. 2428 -2433.